Fuel 117 (2014) 206–217

Contents lists available at ScienceDirect

Fuel

journal homepage: www.elsevier.com/locate/fuel

Understanding the polydisperse behavior of asphaltenes during precipitation

Mohammad Tavakkoli [a,b,*], Sai R. Panuganti [a], Vahid Taghikhani [b], Mahmoud Reza Pishvaie [b], Walter G. Chapman [a]

[a] Department of Chemical and Biomolecular Engineering, Rice University, Houston, USA
[b] Department of Chemical and Petroleum Engineering, Sharif University of Technology, Tehran, Iran

HIGHLIGHTS

- The PC-SAFT equation-of-state is used to study asphaltene phase behavior.
- The effect of asphaltene polydispersity on asphaltene phase behavior is studied.
- Results of monodisperse and polydisperse asphaltenes modeling are compared.
- A wide range of crude oils are considered for the study.
- An explanation for the observed behavior is provided based on Flory–Huggins theory.

ARTICLE INFO

Article history:
Received 28 June 2013
Received in revised form 16 September 2013
Accepted 19 September 2013
Available online 5 October 2013

Keywords:
Asphaltenes
Polydisperse
Phase behavior
PC-SAFT

ABSTRACT

Asphaltenes are a polydisperse fraction of the crude oil, the phase behavior of which is significantly affected by the changes in pressure, temperature and composition. The focus of this study is to model the polydisperse asphaltenes' precipitation onset condition and the amount of precipitate from solvent-diluted crude oils using the Perturbed Chain form of the Statistical Associating Fluid Theory (PC-SAFT) over a wide range of crude oil density. Heavy oil and bitumen production can involve diluting with paraffinic solvents. Different fractions of the polydisperse asphaltenes thus precipitated are predicted and when compared to the experimental data show a remarkable matching for different solvents. A comparison of monodisperse and polydisperse modeling is also performed. This work illustrates the successful application of PC-SAFT for predicting the phase behavior of polydisperse asphaltenes and in particular from heavy oil and bitumen.

1. Introduction

Asphaltenes, a polydisperse mixture of the heaviest and most polarizable fraction of the crude oil; are defined according to their solubility properties as being soluble in aromatic solvents, but insoluble in light paraffin solvents. Asphaltenes are well-known for their tendency to precipitate and deposit during oil production because of changes in pressure, temperature, and composition. It is desirable to prevent or mitigate asphaltene flow assurance problems, because remediation techniques are a significant cost factor. Therefore, as a first step it is necessary to predict the onset and amount of asphaltenes precipitation.

Thermodynamic models to understand the asphaltenes precipitation fall under one of two molecular thermodynamic frameworks, mirroring the two prevalent schools of thought regarding how asphaltenes are stabilized in crude oil. The first approach assumes that asphaltenes are solvated in crude oil and that these asphaltenes will precipitate if the quality of the oil solvent drops below a certain threshold. The Flory–Huggins-regular-solution based models and the equation of state based models are some examples of this approach [1–3]. Thermodynamic models in the second category take a colloidal approach to describe asphaltenes behavior. In this approach resins stabilize the asphaltenes in the crude oil [4,5]. The second approach was beneficial in the early stages of understanding asphaltene behavior. However, aspects like addition of toluene (not a resin) which can redissolve asphaltenes made the asphaltene research community tend towards the solubility approach (first approach).

In this work, the first approach is adopted and a SAFT based equation of state is used to model the asphaltenes behavior [6].

* Corresponding author at: Department of Chemical and Biomolecular Engineering, Rice University, Houston, USA. Tel.: +1 713 348 4900.
E-mail addresses: mohammad.tavakkoli@rice.edu (M. Tavakkoli), sai@rice.edu (S.R. Panuganti), taghikhani@sharif.edu (V. Taghikhani), pishvaie@sharif.edu (M.R. Pishvaie), wgchap@rice.edu (W.G. Chapman).

0016-2361/$ - see front matter © 2013 Elsevier Ltd. All rights reserved.
http://dx.doi.org/10.1016/j.fuel.2013.09.069

Previous work by Ting et al. showed that the phase behavior of asphaltenes is different when considered as monodisperse and polydisperse [7]. Ting et al. considered the effect of asphaltenes' polydispersity for only model oil systems. Although Victorov and Smirnova modeled asphaltenes polydispersity in real crude oil systems, they could not obtain a good match with the presented data [8]. Wang and Buckley presented experimental data showing the effect of dilution ratio on different fractions of asphaltenes [9]. Good knowledge of the polydisperse behavior of the asphaltenes is important because different fractions precipitate in different amounts under different conditions. In this regard, limited modeling work is available in the literature. Hence, this article deals with PC-SAFT modeling of real crude oil systems containing polydisperse asphaltenes. A detailed explanation on their behavior is also presented based on the Flory–Huggins theory.

2. Modeling procedure

The focus of this work is to model the polydisperse asphaltenes based on the experimental data for titration of dead oils with various *n*-alkanes. The PC-SAFT characterization methodology is described elsewhere in detail [10]. Hence, this section discusses only about the asphaltenes and the parameter estimation of this polydisperse fraction.

2.1. Asphaltenes and their sub-fractions

For treating asphaltenes as polydisperse, asphaltenes are split into sub-fractions based on the precipitating solvents used. For example, when *n*-C_{10}, *n*-C_7 and *n*-C_5 are used as the titrating agents, asphaltenes are modeled as *n*-C_{10+} sub-fraction, *n*-C_{7-10} sub-fraction, and *n*-C_{5-7} sub-fraction. Here, the *n*-C_{10+} asphaltene sub-fraction represents *n*-decane insoluble asphaltenes. Asphaltenes from the combination of *n*-C_{10+} and *n*-C_{7-10} sub-fractions represent the *n*-heptane insoluble asphaltenes. Finally, the combination of *n*-C_{10+}, *n*-C_{7-10} and *n*-C_{5-7} sub-fractions represent the *n*-pentane insoluble asphaltenes.

2.2. Asphaltenes' parameter estimation

Asphaltene molecules aggregate forming nano-aggregates even in good solvents such as toluene. Along with polarizability, polarity of the asphaltenes may also play a role in forming the nano-aggregates, but steric effects are thought to prevent further aggregation of asphaltenes in solution [11]. Precipitation is a phenomenon dominated by polarizability creating microdomains of asphaltene rich phase [12]. Because of this, the association term in SAFT can be safely neglected in asphaltenes modeling work.

For every non-associating component, PC-SAFT has just three parameters, the temperature independent diameter of each molecular segment (σ), the number of segments per molecule (m), and the segment–segment dispersion energy (ε/k). When considering a compound which is not well defined like asphaltenes, these three parameters as well as asphaltenes' molecular weight are fit based on experimental data. But, when asphaltenes are considered as polydisperse, the number of parameters increases in multiples of the number of sub-fractions. To reduce the number of parameters, the PC-SAFT parameter correlations for Aromatics + Resins pseudo-component presented by Gonzalez et al. (Table 1) are used in this work to calculate the asphaltenes' parameters [13]. The aromaticity parameter of asphaltenes is kept constant for all the asphaltene sub-fractions of one oil (because the pseudo-components should have the same nature), and only the molecular weight of each sub-fraction along with the aromaticity are fit. The parameter of aromaticity (γ) used in these correlations determines the component's tendency to behave as a poly-nuclear-aromatic ($\gamma = 1$) or as a benzene derivative ($\gamma = 0$).

Table 1
PC-SAFT parameters correlations for asphaltenes.

PC-SAFT Parameter	Correlation
M	$(1-\gamma)\,(0.0223\,Mw + 0.751) + \gamma\,(0.0101\,Mw + 1.7296)$
σ (A)	$(1-\gamma)\,(4.1377 - 38.1483/Mw) + \gamma\,(4.6169 - 93.98/Mw)$
ε/k (K)	$(1-\gamma)\,(0.00436\,Mw + 283.93) + \gamma\,(508 - 234100/(Mw)\text{^}1.5)$

It should be mentioned that in most cases of polydisperse asphaltenes, the correlations in Table 1 give the right values for asphaltene SAFT parameters. But, in some cases like Lagrave oil in Section 3.1, we need to treat the parameter σ as a separate fitting parameter to find a good match. One single value of σ should be used for all asphaltenes' sub-fractions and the correlation in Table 1 gives us a good initial estimate for σ. So in this case, we have one aromaticity and one σ besides molecular weights of asphaltenes' sub-fractions which need to be fitted to reproduce asphaltene instability experimental data. We will see later that even in the case of using the correlation in Table 1 for calculating the parameter σ, the obtained values for all asphaltenes' sub-fractions are equal if one rounds them off to two decimals which is a result of assuming the same aromaticity for each asphaltenes sub-fraction.

3. Results and discussion

3.1. Lagrave oil

3.1.1. Asphaltenes polydispersity

In the experiments performed by Wang, the asphaltenes for Lagrave oil are first separated into various solubility fractions using excess *n*-pentane, *n*-heptane, and *n*-pentadecane precipitants [14]. These sub-fractions are called *n*-C_5 insoluble asphaltenes, *n*-C_7 insoluble asphaltenes, and *n*-C_{15} insoluble asphaltenes, respectively. The asphaltenes instability onsets for mixtures of asphaltene, toluene, and *n*-alkanes (at ambient condition and an asphaltenes/toluene ratio of 1 g per 100 ml toluene) are then measured for each asphaltenes fraction.

Within the PC-SAFT model, polydisperse asphaltenes are modeled as three pseudo-components: *n*-C_{15+} sub-fraction, *n*-C_{7-15} sub-fraction, and *n*-C_{5-7} sub-fraction. The parameters of molecular weight and aromaticity are fit for the *n*-C_{15+} asphaltenes sub-fraction to reproduce the experimental data on the minimum volume fraction precipitant needed to induce asphaltenes instability (φ_v^{ppt}) for mixtures of *n*-C_{15} insoluble asphaltenes, toluene, and various *n*-alkanes. It should be mentioned that the fitting parameters were optimized to match all the experimental data points for all *n*-alkanes. The asphaltenes made from the combination of *n*-C_{15+} and *n*-C_{7-15} sub-fractions represent the *n*-C_7 insoluble asphaltenes. The molecular weight is fit for the *n*-C_{7-15} sub-fraction to reproduce (together with the previously fitted *n*-C_{15+} sub-fraction) the experimental φ_v^{ppt} data for a mixture of *n*-C_7 insoluble asphaltenes, toluene, and *n*-alkane. Finally, the molecular weight parameter of *n*-C_{5-7} sub-fraction is fit so that the combination of the *n*-C_{15+} (previous fit), *n*-C_{7-15} (previous fit), and *n*-C_{5-7} sub-fractions represent the *n*-C_5 insoluble asphaltenes and will reproduce the experimental φ_v^{ppt} data for a mixture of *n*-C_5 insoluble asphaltenes, toluene, and *n*-alkanes.

3.1.2. Parameters

In this section polydisperse asphaltenes are modeled as three pseudo-components, hence four adjustable parameters are used, one aromaticity value and three molecular weights for each of

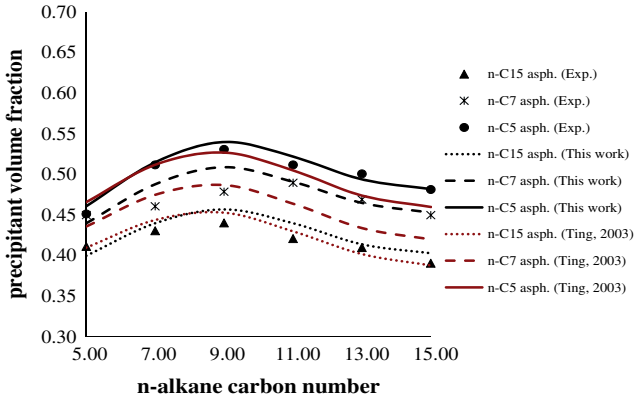

Fig. 1. Comparison of the PC-SAFT modeling results from Ting and the current work with respect to the experimental precipitant volume fraction at asphaltenes instability onset for Lagrave asphaltenes-toluene-*n*-alkane mixtures (20 °C and 1 bar). Experimental data are from Wang [14].

Table 2
PC-SAFT parameters for various asphaltenes sub-fractions of Lagrave oil.

Asphaltenes sub-fractions	Asphaltenes aromaticity (γ)	*Mw* (g/mol)	Wt. %	σ (A)	*M*	ε/k (K)
C_{15+}	0.4	1475	45	4.00	26.84	375.76
C_{7-15}	0.4	1200	30	4.00	22.05	374.44
C_{5-7}	0.4	1150	25	4.00	21.18	374.17

the asphaltenes sub-fractions. Since we are going to investigate just the effect of asphaltene polydispersity and compare it to monodisperse asphaltenes, we kept other parameters affecting asphaltene phase behavior, the same for both cases of polydisperse and monodisperse asphaltenes. Also, to reduce the number of fitted parameters, all binary interaction parameters between asphaltenes and other species are set to zero. The binary interaction parameters, *kij's*, between all species are also set to 0 because SAFT adequately describes the VLE behavior of these systems with zero *kij* [15]. In next sub-sections we will discussed about the effect of *kij's* on model predictions for two real oil systems.

Furthermore, in light of the parameter uniqueness issues discussed by Ting in his Ph.D. thesis (2003), the segment diameters of all asphaltenes pseudo-components (σ) are set to the same value of 4.00 [15], while the other two parameters, *m* and ε/k, are calculated using correlations presented in Table 1. Also, we previously mentioned that for Lagrave oil we need to treat parameter σ as a separate fitting parameter and we found the value of 4.00 for σ will result in a good match between modeling and experimental results. A comparison of the equation of state fitted and the experimental φ_v^{ppt} data is shown in Fig. 1, with the fitted PC-SAFT asphaltenes parameters listed in Table 2. As seen in Table 2, the values of parameters ε/k for different asphaltenes sub-fractions are very close to each other which is a result of assuming the same aromaticity for each asphaltenes sub-fraction. Since we have used the experimental data for Lagrave asphaltenes, not Lagrave oil, the characterization data for Lagrave asphaltenes is presented in this study. For more information about Lagrave oil, kindly refer to reference 14.

For more clarification of Fig. 1, it should be mentioned that the experimental carbon numbers in the legend, i.e. *n*-C_5, *n*-C_7 and *n*-C_{15} asphaltenes, show three different types of asphaltenes, extracted from Lagrave oil using three different *n*-alkanes, i.e. *n*-C_5, *n*-C_7 and *n*-C_{15}, and used for preparation of Lagrave asphaltenes + toluene mixtures. The carbon number on the *x*-axis shows the carbon number of added *n*-alkane to the mixture of Lagrave asphaltenes + toluene to find the instability onset of the solution.

3.1.3. Comparison to previous results

As seen in the Fig. 1, the agreement between PC-SAFT calculated and measured φ_v^{ppt} is remarkable. In the modeling results presented by Ting for the precipitation onsets with *n*-alkane extracted asphaltenes, SAFT did not accurately describe the experimental φ_v^{ppt} data in cases where larger *n*-alkanes (undecane and higher) are used to induce asphaltenes precipitation [15]. Fig. 1 compares the results obtained in this work and those predicted by Ting. The modeling results for *n*-C_{15} asphaltenes, obtained by Ting, show a better match in comparison to this work modeling results. But, for two cases of *n*-C_5 and *n*-C_7 asphaltenes, this work represents a better match. The average error percentages for the modeling results presented by Ting are 2.53%, 4.54% and 1.83% for *n*-C_5, *n*-C_7 and *n*-C_{15} asphaltenes, respectively. The error percentages for this work modeling results are 1.31%, 2.71% and 2.90% for *n*-C_5, *n*-C_7 and *n*-C_{15} asphaltenes, respectively. The average error percentage is calculated using the equation: $\frac{\sum_{i=1}^{n}\|x_i^{exp}-x_i^{model}\|}{n}$. The experimental data for *n*-C_7 asphaltenes in Fig. 1 is different than those from *n*-C_5 and *n*-C_{15} asphaltenes. For the details of experimental procedure as well as the discussion on obtained experimental data, kindly refer to Ref. [14].

It should be mentioned that although we have used less numbers of fitting parameters, the modeling results show a better match in comparison to modeling results obtained by Ting. Ting used three asphaltenes sub-fractions and fitted three molecular weighs, three *m* parameters, three ε/k parameters, and one σ parameter [15]. Also, he fitted the amount of each asphaltenes sub-fraction to reproduce the experimental data on asphaltene instability onset. But, in this study we fitted one aromaticity, one σ parameter and three molecular weights for three asphaltenes sub-fractions. We also fitted the amount of each asphaltenes sub-fraction to reproduce the experimental data on asphaltene instability onset. So, the improvement of this study over the Ting's work is in using less parameters as well as finding a better modeling result with less error percentage in comparison to experimental data.

3.1.4. Maxima

One of the interesting points in Fig. 1 is the existence of a maximum in the curve of the experimental precipitant volume fraction at asphaltenes instability onset versus precipitant agent carbon number. Fig. 1 shows that the PC-SAFT predictions also present this maximum. The onset of precipitation is increasing as the precipitant agent carbon number is increasing up to around *n*-C_9 (around *n*-C_{11} for *n*-C_7 asphaltenes experimental data). After *n*-C_9, the precipitant volume fraction at asphaltenes instability onset will decrease by increasing *n*-alkane carbon number. This observation on the trend of precipitation onset data is in line with Wiehe et al. who discussed the solubility parameter difference between *n*-paraffin and asphaltenes in the oil and also the ratio of the molar volume of asphaltenes to the molar volume of *n*-paraffin [16].

Upon increasing the carbon number of *n*-alkane that is blended with oil, the solubility parameter difference between *n*-paraffin and asphaltenes in the oil becomes smaller and the ratio of the molar volume of asphaltenes to the molar volume of *n*-paraffin in the entropy of mixing becomes smaller. Both of these effects decrease the free energy of mixing and make the *n*-alkane and asphaltenes more compatible. This is why, at small-carbon-number *n*-paraffins, the volume of *n*-paraffin at the flocculation point increases as the *n*-paraffin carbon number increases. However, as the carbon number of the *n*-paraffin increases, the rate of increase of the solubility parameter decreases, while the molar volume increases linearly. Thus, the enthalpy of mixing increases as the molar volume of *n*-

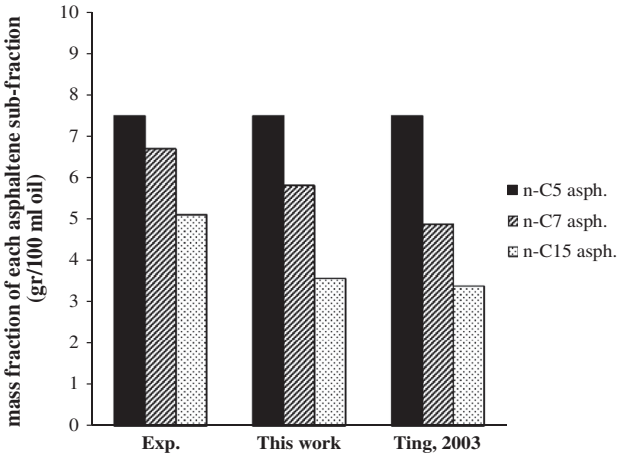

Fig. 2. Comparison of mass distribution of each asphaltenes sub-fraction in Lagrave oil. Experimental data are from Wang [14].

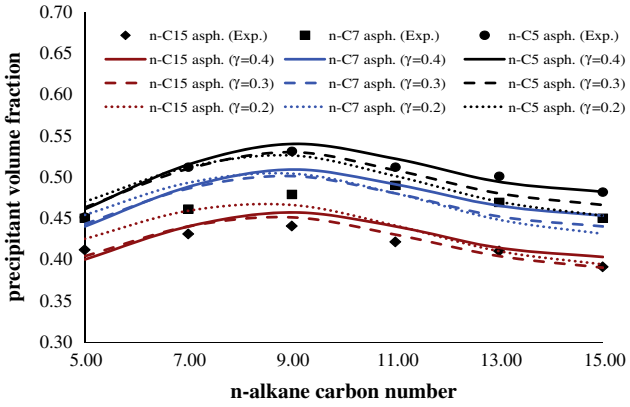

Fig. 3. Comparison of the PC-SAFT equation of state fitted for different values of asphaltenes aromaticity and the experimental precipitant volume fraction at asphaltenes instability onset for Lagrave asphaltenes-toluene-n-alkane mixtures (20 °C and 1 bar). Experimental data are from Wang [14].

Table 3
PC-SAFT parameters for various asphaltenes sub-fractions at different values of asphaltenes aromaticity.

Asphaltenes sub-fractions	Asphaltenes aromaticity (γ)	*Mw* (g/mol)	Wt. %	σ (A)	M	ε/k (K)
C_{15+}	0.4	1475	45	4.00	26.84	375.76
C_{7-15}	0.4	1200	30	4.00	22.05	374.44
C_{5-7}	0.4	1150	25	4.00	21.18	374.17
C_{15+}	0.3	2280	45	4.00	43.54	357.46
C_{7-15}	0.3	1500	30	4.00	29.00	354.52
C_{5-7}	0.3	1450	25	4.00	28.07	354.30
C_{15+}	0.2	3800	45	4.00	76.41	341.80
C_{7-15}	0.2	2200	30	4.00	44.64	335.96
C_{5-7}	0.2	2100	25	4.00	42.65	335.58

paraffin increases and soon overcomes the effect of the decreasing solubility parameter difference between *n*-paraffin and asphaltenes in the oil. This causes the free energy of mixing to increase with increasing *n*-paraffin carbon number at higher carbon numbers, and results in decrease in the volume of *n*-paraffin at the flocculation point, relative to increasing *n*-paraffin carbon number. The consequence is a maximum in the volume of *n*-paraffin at the flocculation point as one increase the carbon number of *n*-paraffin blended with an oil-containing asphaltenes.

3.1.5. Mass distribution

A comparison of the PC-SAFT predicted and measured mass distribution of the asphaltenes sub-fractions is shown in Fig. 2. For the column labeled "experimental", the mass of each asphaltenes subfraction is inferred from the difference in the measured amount of asphaltenes precipitated with different precipitants. Wang used excess amount of *n*-pentane, *n*-heptane, and *n*-pentadecane precipitants to separate asphaltenes from Lagrave oil and measure the amount of precipitated asphaltenes [14]. Within the PC-SAFT model, the amount of each asphaltenes sub-fraction is optimized to fit the experimental φ_v^{ppt} data in Fig. 1. It is interesting to note that the modeled mass distribution in this work is closer to experimentally measured values in comparison to those predicted by Ting [15]. For Lagrave oil, it is necessary to say that we could not find a good match in the case of using the experimental mass of each asphaltenes sub-fraction and the reason will be discussed in the next paragraph. But, for the other oils in this study, asphaltenes will be divided into a number of sub-fractions based on the experimental data for total amount of precipitated asphaltenes using different *n*-alkanes.

The amount of high molecular weight asphaltenes (n-C_{15} asphaltenes) could not be matched as observed from Fig. 2. This can be attributed to several factors. Experimentally, the measured amount of asphaltenes precipitated may contain not only asphaltenes that should precipitate with the precipitant used, but also small amounts of entrained resins, oil, and other asphaltenes fractions. Variations in the amount of asphaltenes precipitated exist even for the same oil using the same extraction procedure. On the modeling side, because there are insufficient data to uniquely fit all of the model parameters for polydisperse asphaltenes, certain approximations have to be made. For instance, the segment diameter of all asphaltenes sub-fractions is set to 4.00 Angstroms, because we could not find a good match using the correlation in Table 1 for parameter σ.

3.1.6. Sensitivity analyses

To investigate the effect of asphaltenes' aromaticity on phase behavior, different sets of asphaltene aromaticity with molecular weight of the sub-fractions are fit to experimental φ_v^{ppt} data shown in Fig. 1. Table 3 shows the asphaltenes parameters fitted to experimental φ_v^{ppt} data at different values of asphaltenes aromaticity.

Fig. 3 shows a comparison of the equation of state fitted with different values for asphaltenes aromaticity and the experimental φ_v^{ppt} data. A reasonable match is obtained when aromaticity value is in the range of 0.2–0.4 for Lagrave asphaltenes. From Table 3, one may conclude that there is wide range for asphaltene SAFT parameters *m* and ε/k. Here, it is necessary to say that the issue of uniqueness of the asphaltene SAFT parameters has already been investigated by Ting [15]. Different values for asphaltene molecular weight and aromaticity result in various asphaltene SAFT parameters. So, it is possible to find reasonable results using different sets of fitting parameters as shown by Ting (2003). The phase behavior calculated using these different sets of asphaltene parameters are similar and we believe the effects of the nonuniqueness of asphaltenes SAFT parameters on asphaltene phase behavior in oil should be small [15]. For the best fit, one needs to choose the set of fitting parameters which shows the minimum error percentage between modeling results and experimental data. For Lagrave asphaltenes, the best fit happens when the value of 0.4 is selected for asphaltene aromaticity.

When aromaticity is decreased, higher molecular weights of asphaltenes sub-fractions are needed to obtain a reasonable match with the experimental data. Also, it should be mentioned that in all

cases the weight percent of asphaltenes fractions is: 45%, 30% and 25% for C_{15+}, C_{7-15} and C_{5-7} sub-fractions, respectively.

In the above cases with different values of asphaltenes aromaticity and molecular weight, asphaltenes PC-SAFT parameters are checked to be in the acceptable range (between pure saturates and pure poly-nuclear-aromatics). Also, in each case the asphaltenes solubility parameter calculated using the PC-SAFT equation of state is found to be in the range 19 and 24 $MPa^{0.5}$ reported in the literature [15]. The asphaltene molecular weight is still under debate in the literature [17]. Asphaltenes' selfassociation along with asphaltenes' polydispersity are the reasons why there is no range in the reported molecular weight and structural properties of asphaltenes.

3.1.6.1. Asphaltene aromaticity. To see the effect of asphaltenes aromaticity on the asphaltene precipitated amount, model oil system 1 is defined consisting of monodisperse Lagrave *n*-C_{15+} asphaltenes, the PC-SAFT parameters of which are fit to the experimental φ_v^{ppt} using various values for asphaltene aromaticity. In this model system 1, toluene is used as the model oil and the asphaltenes/toluene ratio while modeling is taken the same as the experiment by Wang, 1 g/100 ml [14]. Standard conditions of 20 °C and 1 bar are assumed. Fig. 4 shows the amount of precipitated asphaltenes from model system 1 predicted by PC-SAFT using the parameters in the Table 3. N-pentadecane is used as the precipitating agent. It can be found from Fig. 4 that lower values for asphaltenes aromaticity will result in more asphaltenes being precipitated. Also, asphaltenes re-dissolution begins at lower precipitant volume fractions and with a higher re-dissolution amount when higher values for asphaltenes aromaticity and therefore lower values for molecular weight are used. To understand better the modeling results presented in Fig. 4, precipitant dilution ratio is used in Fig. 5 instead of precipitant volume fraction. Dilution ratio is based on the volume of precipitating agent in cc per 1 g of original oil. It should be mentioned that the format of Fig. 5 will be used for many other figures in the present paper because in many cases we need to compare the modeling results at high amount of added precipitant agent. Also, this format is the common format used in both industrial and academic applications [1,18].

Higher asphaltenes aromaticity means that the nature of asphaltenes in the system is closer to poly-nuclear-aromatics and as a result they are more incompatible with the maltenes in the crude oil. We would expect that higher asphaltenes aromaticity would result in more asphaltene precipitating which is not in line with the modeling results presented in Figs. 4 and 5. The reason is that when higher asphaltenes aromaticity is used, a lower value for asphaltenes molecular weight is needed to obtain a reasonable match with experimental onset data. So, here the effects of both asphaltenes aromaticity and asphaltenes molecular weight are important. In the following paragraphs the contributions of asphaltenes aromaticity and molecular weight in the predicted precipitation amount is discussed. It is necessary to say that if one increases asphaltene aromaticity while the value of asphaltene molecular weight is constant, the modeling results will show more amounts of precipitated asphaltenes as well as a lower dilution ratio for asphaltene precipitation onset. The same result can be seen for increasing asphaltene molecular weight while the value of asphaltene aromaticity is constant.

3.1.7. Molar volume and solubility parameter

Table 4 presents the values of asphaltenes solubility parameter and molar volume, calculated by PC-SAFT, for C_{15+} asphaltenes presented in Table 3. Table 4 shows that the asphaltenes solubility parameter increases with aromaticity and the molar volume increases as molecular weight increases. To understand the contributions of both asphaltenes molar volume and solubility parameter in the amount of precipitation, the Flory–Huggins theory is used.

It is necessary to say that asphaltene aromaticity and molecular weight control the values of asphaltene SAFT parameters. These SAFT parameters can be used for calculating asphaltenes solubility parameter and molar volume by PC-SAFT equation of state. So, we are relating asphaltene aromaticity and molecular weight to asphaltene solubility parameter and molar volume and one may find the effect of aromaticity and molecular weight by investigating the effect of solubility parameter and molar volume. The Flory–Huggins theory may give us a good insight into the effect of solubility parameter and molar volume.

For any two phases at equilibrium, the fugacities of each component in existing phases are equal. For liquid–liquid equilibrium, the equilibrium ratio, K_i can be written as

$$K_i^{HL} = \frac{x_i^H}{x_i^L} = \exp\left(\ln\left(\frac{v_i^L}{v_m^L}\right) - \frac{v_i^L}{v_m^L} + \frac{v_i^L}{RT}\left(\delta_i^L - \delta_m^L\right)^2 - \ln\left(\frac{v_i^H}{v_m^H}\right) + \frac{v_i^H}{v_m^H} - \frac{v_i^H}{RT}\left(\delta_i^H - \delta_m^H\right)^2\right) \quad (1)$$

where i is the component, L and H are the asphaltenes lean and asphaltenes rich phases, respectively, x is the mole fraction, v is the molar volume, R is the universal gas constant, T is the absolute temperature, the subscript m stands for the mixture, and δ is the

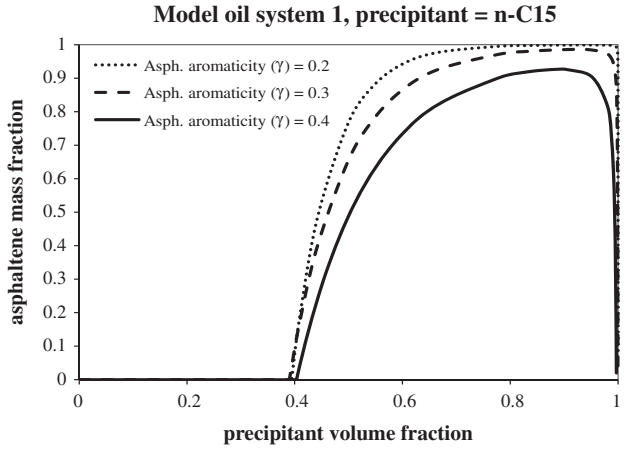

Fig. 4. Precipitated asphaltenes mass fraction versus *n*-pentadecane volume fraction at different values of asphaltenes aromaticity for the model oil system 1.

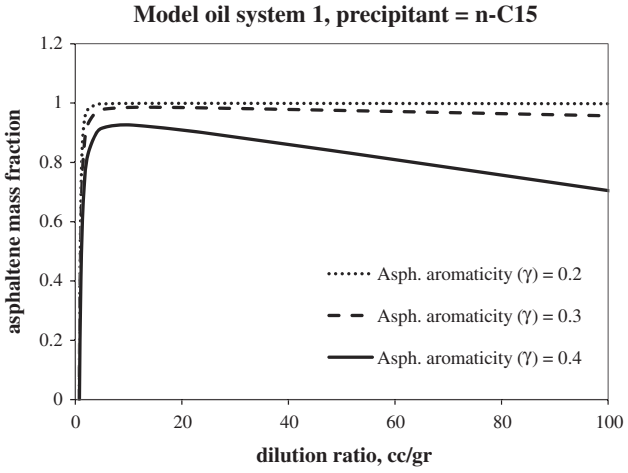

Fig. 5. Precipitated asphaltenes mass fraction versus *n*-pentadecane dilution ratio, cc/g, at different values of asphaltenes aromaticity for the model oil system 1.

Table 4
Values of solubility parameter and molar volume for C_{15+} asphaltenes sub-fraction at different values of asphaltenes aromaticity calculated by PC-SAFT.

Asphaltenes	Asphaltenes aromaticity (γ)	Molecular weight (g/mol)	Molar volume (cm^3/mol)	Solubility parameter ($MPa^{0.5}$)
C_{15+}	0.4	1475	1069.06	23.29
C_{15+}	0.3	2280	1747.48	22.49
C_{15+}	0.2	3800	3091.05	21.76

solubility parameter. The general derivation of Eq. (1) can be found elsewhere [2].

Assuming that only asphaltenes partition to asphaltenes rich phase, the above equation will result in the same equation proposed by Hirschberg et al. for modeling asphaltenes precipitation by combining the Flory–Huggins theory for polymer solution and Hildebrand solubility concept [1]. But, this assumption is not accurate for asphaltenes thermodynamic modeling using PC-SAFT, because although asphaltenes rich phase consist mainly asphaltenes, there are considerable amount of saturates as well as resins and aromatics in this phase [19]. Rearrangement of Eq. (1) results in

$$K_i^{HL} = \frac{x_i^H}{x_i^L} = \exp\left(\left[\ln\left(\frac{v_i^L}{v_m^L}\right) - \ln\left(\frac{v_i^H}{v_m^H}\right)\right] - \left(\frac{v_i^L}{v_m^L} - \frac{v_i^H}{v_m^H}\right)(\chi^L - \chi^H)\right) \tag{2}$$

where χ is the Flory–Huggins interaction parameter

$$\chi = \frac{v_i}{RT}(\delta_i - \delta_m)^2 \tag{3}$$

Based on Eq. (2), when $(\chi^L - \chi^H)$, increases the amount of precipitation will increase, while $\left(\frac{v_i^L}{v_m^L} - \frac{v_i^H}{v_m^H}\right)$ has a reverse effect. Figs. 6 and 7 represent the PC-SAFT calculated values for two expressions $\left(\frac{v_i^L}{v_m^L} - \frac{v_i^H}{v_m^H}\right)$ and $(\chi^L - \chi^H)$, respectively, for the three cases presented in Table 4.

From Figs. 6 and 7 it can be concluded that for the case of $\gamma = 0.2$ and $Mw = 3800$, both molar volume ratio difference and value of Flory–Huggins interaction parameter difference are more for this case in which the effect of Flory–Huggins interaction parameter difference is higher than the molar volume ratio difference and would result in more asphaltenes precipitation for the case of $\gamma = 0.2$ and $Mw = 3800$. In other words, although asphaltenes solubility parameter has a lower value for $\gamma = 0.2$ and $Mw = 3800$, the molar volume for this case is more than two other cases which results in a higher value for the Flory–Huggins interaction parameter and this case shows less asphaltenes re-dissolution by increasing precipitant volume fraction.

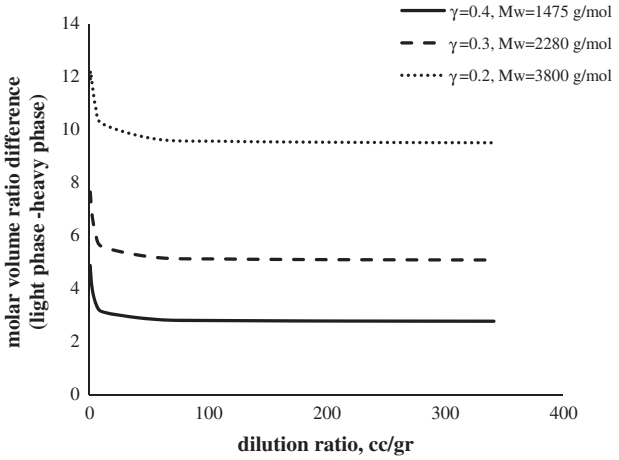

Fig. 6. Molar volume ratio difference between light and heavy phases calculated using PC-SAFT versus *n*-pentadecane dilution ratio at different values of asphaltenes aromaticity and molecular weight.

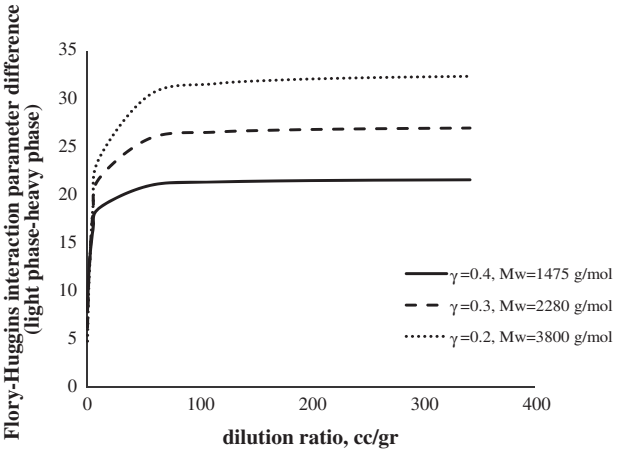

Fig. 7. Flory–Huggins interaction parameter difference between light and heavy phases calculated using PC-SAFT versus *n*-pentadecane dilution ratio at different values of asphaltenes aromaticity and molecular weight.

3.1.8. Monodisperse vs polydisperse

To investigate the roles of polydispersity on asphaltenes phase behavior, the solubility behavior of two model oil mixtures with monodisperse and polydisperse asphaltenes are compared. In these model systems 2 and 3, toluene is used as the model oil (with different amounts of *n*-alkane precipitants added) and the asphaltenes' parameters are fit to experimental φ_v^{ppt} data for Lagrave asphaltenes. The asphaltenes/toluene ratio while modeling is taken the same as the experiment by Wang (2000), 1 g/100 ml. Standard conditions of 20 °C and 1 bar are assumed for both the model systems. Model system 2 is a monodisperse system consisting of Lagrave *n*-C_5 asphaltenes, the PC-SAFT parameters of which are fit to the experimental φ_v^{ppt} for *n*-C_5 asphaltenes in Fig. 1. The aromaticity and molecular weight of these monodisperse *n*-C_5 asphaltenes are 0.4 and 1375, respectively. Also, the value of 4.00 was used for parameter σ. In model system 3, polydisperse asphaltenes with 3 subfractions: C_{5-7}, C_{7-15} and C_{15+} are used. The weight percent of asphaltenes fractions is: 45%, 30% and 25% (C_{15+}, C_{7-15} and C_{5-7}) and the PC-SAFT parameters for each asphaltenes subfraction are fit to the experimental φ_v^{ppt} data of the fractionated asphaltenes. See Table 2 for asphaltenes sub-fractions parameters. All binary interaction parameters between all species used in the PC-SAFT calculations in this section are set to zero.

The effects of *n*-alkane addition on the amount of asphaltenes precipitated at 20 °C and 1 bar for the two model oils are shown in Figs. 8 and 9. The *y*-axis shows the precipitated asphaltene amount as a fraction of total asphaltene content of the oil. Since same asphaltenes have been used in both model systems and the PC-SAFT parameters of asphaltenes are fit to the experimental φ_v^{ppt} data, we can see the same asphaltene precipitation onset in both cases of monodisperse and polydisperse asphaltenes. However, a change in the amount of precipitated asphaltenes vs. precipitant volume fraction can be seen for the case of polydisperse

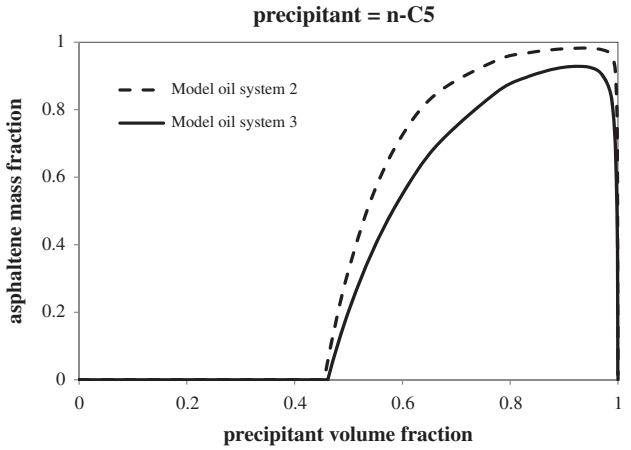

Fig. 8. Asphaltenes mass fraction versus *n*-pentane volume fraction for model oil system 2 (monodisperse asphaltenes) and model oil system 3 (polydisperse asphaltenes) at 20 °C and 1 bar. Model oil contains 1 gram of Lagrave oil asphaltenes in 100 ml toluene.

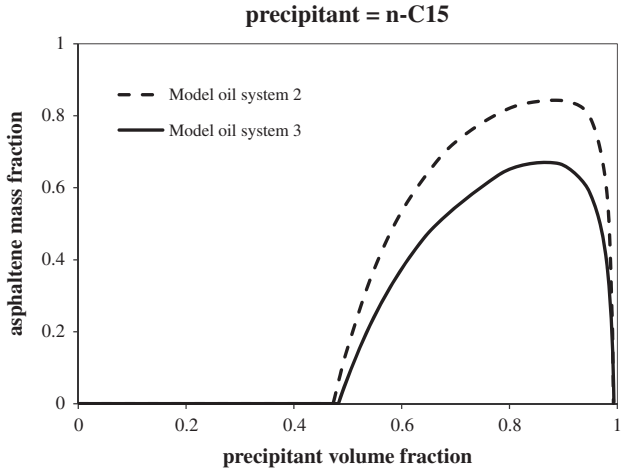

Fig. 9. Asphaltenes mass fraction versus *n*-pentadecane volume fraction for model oil system 2 (monodisperse asphaltenes) and model oil system 3 (polydisperse asphaltenes) at 20 °C and 1 bar. Model oil contains 1 gram of Lagrave oil asphaltenes in 100 ml toluene.

asphaltenes. By treating asphaltenes as a polydisperse species, the amount of asphaltenes precipitated increases more gradually with precipitant addition. Also, the total amount of precipitated asphaltenes in polydisperse system is less than the total precipitated amount in monodisperse system. In a polydisperse system, some amount of lower molecular weight asphaltenes (C_{5-7} and C_{7-15}) exists in the mixture, and a significant amount of asphaltenes will stay in solution even at high precipitant volume fractions. Thus, more asphaltenes can be precipitated using lower molecular weight *n*-alkanes.

Asphaltene redissolution at high dilution ratios is a phenomenon reported in literature [9]. It can be seen from Figs. 8 and 9 that asphaltenes re-dissolution begins at lower precipitant volume fractions and with a higher re-dissolution amount for polydisperse model system (system 3). Existence of low molecular weight asphaltenes sub-fractions (C_{5-7} and C_{7-15}) which can dissolve in the system better than high molecular weight asphaltenes (C_{15+}) is the reason for this re-dissolution. Also, the amount of re-dissolution is more for higher carbon number precipitant agents, because they are better solvents for asphaltenes than lower carbon number *n*-alkanes.

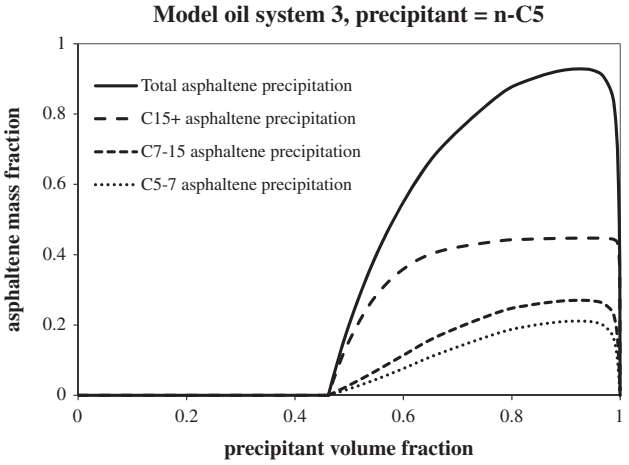

Fig. 10. Distribution of the asphaltenes sub-fractions in the precipitated phase as a function of *n*-pentane volume fraction in the model oil system 3 (polydisperse asphaltenes).

3.1.9. Fractions of individual precipitation

To see the role of each asphaltenes sub-fraction in the total amount of precipitated asphaltenes, plots of the mass distribution of polydisperse asphaltenes sub-fractions as a function of precipitant volume fraction are shown in Figs. 10 and 11. From the Figs. 10 and 11 it is observed that near the initial asphaltenes instability onset, the precipitated phase is composed mostly of the heaviest asphaltenes fractions (*n*-C_{15+} sub-fraction). As the amount of precipitant is increased further, lower molecular weight asphaltenes will also precipitate. From Figs. 10 and 11, one can also see that the amount of re-dissolution is more for higher carbon number precipitant agents following the explanation earlier in this section. Unfortunately there is no experimental data on the precipitated amount of each asphaltenes sub-fraction in the literature to compare with modeling results obtained by PC-SAFT. Part of the reason is the difficulties in extracting asphaltenes sub-fractions from crude oils. Hence, the results presented here for the role of each asphaltenes sub-fraction are theoretical predictions.

3.2. Iranian oil

The model results discussed thus far are based on the asphaltenes data for Lagrave oil. As further tests/proof of general applicability of the model, we will compare with experimental data for several other oils including both light and heavy crudes.

Titration experimental results presented by Hirschberg et al. (1984) are one of the well-known asphaltene studies available in the literature [1]. The oil used is an Iranian crude oil with an *n*-heptane asphaltenes content of 1.9 weight percentage in the stock tank oil. Table 5 presents PVT properties of this crude. Table 6 shows the results of titration experiments performed on stock tank oil presented in Table 5.

For modeling of Iranian oil titration experiments, asphaltenes are divided into three sub-fractions: *n*-C_{5-7}, *n*-C_{7-10} and *n*-C_{10+} asphaltenes, based on the experimental amount of *n*-C_5, *n*-C_7 and *n*-C_{10} asphaltenes. These experimental amounts were measured by adding excess amount of *n*-alkane to the tank oil and then filtering the mixture with 0.45 micrometer filter paper and finally washing the filter paper with hot *n*-heptane [1]. Accurate amount of precipitation prediction was not possible using only one asphaltene fraction, i.e. *n*-C_5 asphaltenes for all the titration experiments presented in Table 6. Hence, using polydisperse asphaltenes is the first key point for modeling of these titration experiments.

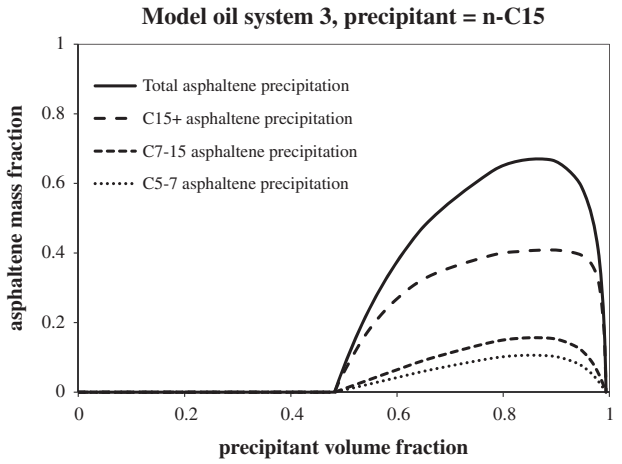

Fig. 11. Distribution of the asphaltenes sub-fractions in the precipitated phase as a function of *n*-pentadecane volume fraction in the model oil system 3 (polydisperse asphaltenes).

Table 5
Iranian oil composition and PVT properties [1].

Component	Composition (mol%)
Methane	0.10
Ethane	0.48
Propane	2.05
i-Butane	0.88
n-Butane	3.16
i-Pentane	1.93
n-Pentane	2.58
Hexane	4.32
Heptane plus	84.5
Saturates (mol%)	50
Aromatics (mol%)	25
n-C_7 asphaltenes (wt%)	1.9
n-C_5 asphaltenes (wt%)	3.9
Asphaltenes + resins (wt%)	18
Molecular weight	221.5
Density (g/cc)	0.873

Table 6
Iranian stock tank oil titration results [1].

Dilution Ratio (cc diluent/g tank oil)	n-C_5	n-C_7	n-C_{10}	n-C_{12}	n-C_{16}
1.0	–	–	–	–	Onset
1.3	–	–	–	Onset	–[b]
1.4	–	Onset	Onset	–[b]	
5	–[a]	1.53	1.34		
10	3.61	1.82	1.45		
20	3.79	1.89	1.5		
50	3.87	1.87			

[a] Onset of flocculation not determined.
[b] Amount of precipitation not determined.

Table 7 presents the characterization results rounded off to two decimals for the Iranian oil using the PC-SAFT methodology. Being dead oil, there is no gas component in the system. The aromaticity value for Aromatics + Resins component is 0.38 and is fitted to the experimental stock tank oil density. The experimental value for stock tank oil density, 0.873 g/cc and the fitted value, 0.872 g/cc are well matched. The aromaticity value for asphaltenes as well as molecular weights of different asphaltenes fractions are fitted to the experimental data for both onset and amount of precipitation. A comparison of the equation of state fitted and the experimental data for onset and amount of precipitation are shown in Figs. 12 and 13, respectively. The *x*-axis in Fig. 12 shows the carbon number for the added precipitant agent.

Titration experiments presented by Hirschberg et al. contains asphaltenes onset of precipitation data with four different *n*-alkanes as well as precipitation amount for three different titrating agents. The PC-SAFT fitted parameters for all these experimental results are: molecular weights of the three asphaltenes sub-fractions and the aromaticity value for asphaltenes component. These four parameters are fit to match simultaneously all experimental data points for onset and amount of precipitation using different titration agents. The only parameter that can help us to handle each titration experiment individually is the binary interaction parameter, *kij*, between asphaltene component and *n*-alkane. The *kij*'s for dead oil, between Saturates, Aromatics + Resins, Asphaltenes and different *n*-alkanes, presented by Gonzalez are used in this work [20]. The *kij*'s between asphaltenes and other components are equal to the *kij*s between Aromatics + Resins and the other components, as presented by Gonzalez. By slightly changing the *kij* between each *n*-alkane and asphaltenes component, one can find a better match for both onset and amount of precipitation. The *kij* between asphaltenes and saturates controls the onset of precipitation as well as the shape of the curve right after the precipitation onset. If one increases the value for the *kij* between asphaltenes and saturates, the modeling results will show a higher slope for the yield curve, right after the onset of precipitation. Also, the modeling results will demonstrate a lower dilution ratio of the precipitant agent for the asphaltene precipitation onset. Thus the *kij* between asphaltenes and saturates is also a matching parameter besides previously mentioned fitting parameters, molecular weights of three asphaltenes sub-fractions and aromaticity value for asphaltenes component. Table 8 presents the binary interaction parameters between all components used for modeling of the Hirschberg titration experiments.

3.3. Heavy oil modeling

In this section, the procedure used for predicting the instability onset data and for modeling the titration experiments of model and light oils is used for modeling of titration experiments for heavy crudes and bitumens available in the literature. The titration experimental results for heavy oils from different sources, Canada, Venezuela, Russia, and Indonesia, presented by Sabbagh et al. are used in this section [21]. Table 9 demonstrates the SARA analysis of these bitumens and heavy oils and measured molar mass and density of each fraction.

Table 7
Characterized Iranian stock tank oil as a combination of five pseudo-components and their PC-SAFT parameters.

Component	*Mw* (g/mol)	Mass fraction	σ (A)	*M*	ε/k (K)
Saturates	207.43	0.468	3.92	6.17	259.32
Aromatics + Resins (γ = 0.38)	219.44	0.493	4.05	4.99	342.30
C_{10+} Asphaltenes (γ = 0.2)	4307.22	0.015	4.22	86.49	343.60
C_{7-10} Asphaltenes (γ = 0.2)	2950.00	0.004	4.22	59.53	338.74
C_{5-7} Asphaltenes (γ = 0.2)	2900.00	0.020	4.22	58.54	338.56

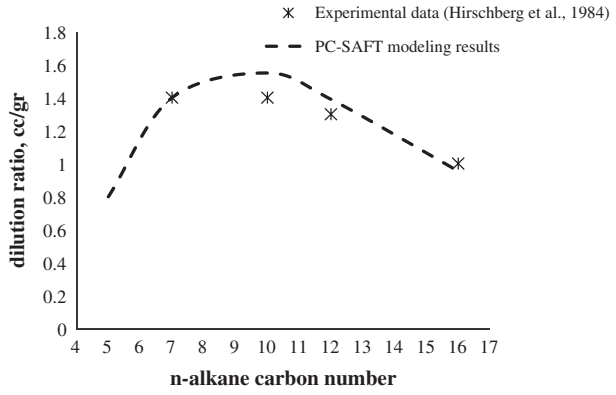

Fig. 12. Comparison of the PC-SAFT equation of state fitted and the asphaltenes instability onset experimental data for Iranian stock tank oil.

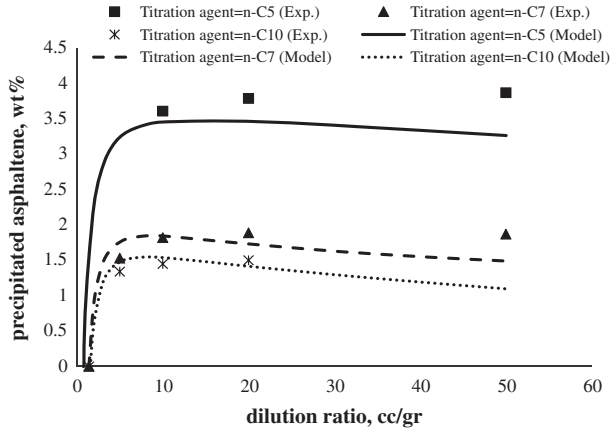

Fig. 13. Comparison of the PC-SAFT equation of state fitted and the experimental amount of precipitated asphaltenes for Iranian stock tank oil. Experimental data from Hirschberg et al. [1].

For modeling of heavy oils in Table 9, asphaltenes fraction in the characterization process is divided into three sub-fractions for the oil from Canada and two sub-fractions for the other three oils, based on the experimental data for total amount of precipitated asphaltenes using different *n*-alkanes. These experimental amounts were measured by addition of excess *n*-alkane to the heavy crude [21].

The molecular weights for saturates, aromatics and resins of all four oils are available, and there is no need to calculate them during the characterization process. The composition data of the crude oils are not available; hence the aromatics and resins fractions could not be combined and are left as individual pseudo-components. The correlations in Table 1 are used for predicting the PC-SAFT parameters of aromatics and resins, using a single aromaticity value for both of them. For asphaltenes fraction, the measured molecular weights are not used for modeling purpose and are treated as a matching parameter for each sub-fraction. When treating asphaltenes as polydisperse, we need the molecular weights for each asphaltenes' sub-fraction which are not available in Table 9.

Table 10 presents the parameters used for modeling of heavy oils and bitumens in Table 9. For each crude oil, the aromaticity value for aromatics and resins components is fitted to the experimental stock tank oil density. The aromaticity values for asphaltenes as well as molecular weights of different asphaltenes fractions are fitted to the experimental data for amount of precipitation. Table 11 shows the asphaltenes' PC-SAFT parameters to the nearest second decimal.

Table 12 compares experimental values and modeling results for the stock tank oil density showing a good agreement (maximum error is less than 2%). A comparison of the equation of state fitted and the experimental data for heavy oils and bitumens from Venezuela, Canada, Russia and Indonesia are shown in Figs. 14–17 respectively. In each case there is a good agreement for the amount of asphaltenes precipitated upon dilution with different precipitants.

From Tables 10 and 12, one can understand that both asphaltenes aromaticity, and aromatics and resins aromaticity decrease

Table 9
SARA analysis of bitumens and heavy oils from Venezuela, Canada, Russia and Indonesia, and the measured molar mass and density of each fraction.

Heavy oil fraction	Content (wt%)	Density (kg/m^3)	Molar mass (g/mol)
Venezuela			
Saturates	20.5	882	400
Aromatics	38.0	997	508
Resins	19.6	1052	1090
Asphaltenes	21.8	1193	7662
Solids	0.1		
Canada			
Saturates	23.1	876	482
Aromatics	41.7	997	537
Resins	19.5	1039	859
Asphaltenes	15.3	1181	6660
Solids	0.4		
Russia			
Saturates	25.0	853	361
Aromatics	31.1	972	450
Resins	37.1	1066	1108
Asphaltenes	6.8	1192	7065
Solids	0.0		
Indonesia			
Saturates	23.2	877	498
Aromatics	33.9	960	544
Resins	38.2	1007	1070
Asphaltenes	4.7	1132	4635
Solids	0.0		

Table 8
Binary interaction parameters used for modeling of Iranian stock tank oil.

Component	n-C_5	n-C_7	n-C_{10}	n-C_{12}	n-C_{16}	Saturates	A + R	C_{5-7} Asph.	C_{7-10} Asph.	C_{10+} asph.
n-C_5	0									
n-C_7	0	0								
n-C_{10}	0	0	0							
n-C_{12}	0	0	0	0						
n-C_{16}	0	0	0	0	0					
Saturates	0	0	0	0	0	0				
A + R	0.007	0.0065	0.006	0.006	0.005	0.007	0			
C_{5-7} Asph.	0.008	0.0065	0.006	0.005	0.005	0.003	0	0		
C_{7-10} Asph.	0.008	0.0065	0.006	0.005	0.005	0.003	0	0	0	
C_{10+} Asph.	0.008	0.0065	0.006	0.005	0.005	0.003	0	0	0	0

Table 10
Aromaticity values for aromatics, resins and asphaltenes pseudo-components as well as various asphaltenes sub-fractions molecular weight used for modeling of bitumens and heavy oils presented in Table 9.

Heavy oil source	Aromatics and resins aromaticity	Asphaltenes aromaticity	C_{5-7} Asph. *Mw* (g/mol)	C_{5-6} Asph. *Mw* (g/mol)	C_{6-7} Asph. *Mw* (g/mol)	C_{7+} Asph. *Mw* (g/mol)
Venezuela	0.3	0.4	2500	–	–	2600
Canada	0.25	0.3	–	3600	3650	3700
Russia	0.23	0.2	4700	–	–	5600
Indonesia	0.22	0.2	4100	–	–	4300

Table 11
Asphaltene PC-SAFT parameters obtained by using the aromaticity and molecular weight from Table 10 in the equations presented in Table 1.

Heavy oil source	Asphaltene fraction	σ (A)	*m*	ε/k (K)
Venezuela	*n*-C_{5-7}	4.30	44.69	379.34
	n-C_{7+}	4.30	46.43	379.65
Canada	*n*-C_{5-6}	4.26	68.14	361.81
	n-C_{6-7}	4.26	69.08	361.97
	n-C_{7+}	4.26	70.01	362.13
Russia	*n*-C_{5-7}	4.22	94.28	344.99
	n-C_{7+}	4.22	112.16	348.16
Indonesia	*n*-C_{5-7}	4.22	92.30	344.63
	n-C_{7+}	4.22	96.27	345.34

when stock tank oil density decreases. Higher aromaticity for correlations in Table 1 shows behavior closer to poly-nuclear-aromatics, and so a crude oil with higher aromaticity contains heavier components. It can be found that as asphaltenes content of heavy oils in Table 9 decreases, the fluid density decreases and modeling results also show a decreasing trend for asphaltenes aromaticity.

It is still unknown how to relate aromaticity parameter to physical properties of a crude oil. It should be mentioned that we used two aromaticity parameters in this study: aromaticity of Aromatics + Resins component and Asphaltenes' aromaticity. It would be great if we can relate these two parameters to the crude oil specifications and its asphaltenes' physical properties, instead of just fitting them based on the experimental data, and so one could improve the predictive nature of the model. To do that, more experiments and modeling studies need to be done. For instance, given the exact values for molecular weight of asphaltenes, one can focus on the values of aromaticity parameters because asphaltenes molecular weight and aromaticity are two related parameters in the modeling of asphaltenes phase behavior.

A key point for modeling of heavy oils presented in Table 9 is using zero binary interaction parameters (*kij*) for asphaltenes, aromatics and resins components, except for *kij* between asphaltenes and saturates which needs to be a negative value. Negative *kij* values for asphaltenes are used by Sabbagh et al. to model the same crude oils using the Peng–Robinson equation of state [21]. They used zero *kij* values for all other components. Also, Panuganti et al. used negative value for *kij* between asphaltenes and saturates for modeling asphaltenes phase behavior using PC-SAFT [10]. Table 13 represents the values for *kij* parameters between asphaltenes and saturates components for all heavy oils and bitumens presented in Table 9. A single value is used for *kij* parameter between saturates and all asphaltenes sub-fractions. This value strongly controls the onset of precipitation as well as the shape of the curve right after precipitation onset.

A point which is learned from modeling of light oils versus heavy oils is the difference in the values of binary interaction parameters used to find a reasonable match. The values for *kij* parameters for light crudes are chosen from the available values in literature which inturn were determined using VLE experimental data. But,

Table 12
Comparison of experimental stock tank oil density and modeled density using PC-SAFT. Experimental values are from Sabbagh et al. [21].

Heavy oil source	Experimental stock tank oil density (g/cc)	Modeled stock tank oil density (g/cc)
Venezuela	1.016	0.998
Canada	0.996	0.985
Russia	0.982	0.970
Indonesia	0.963	0.962

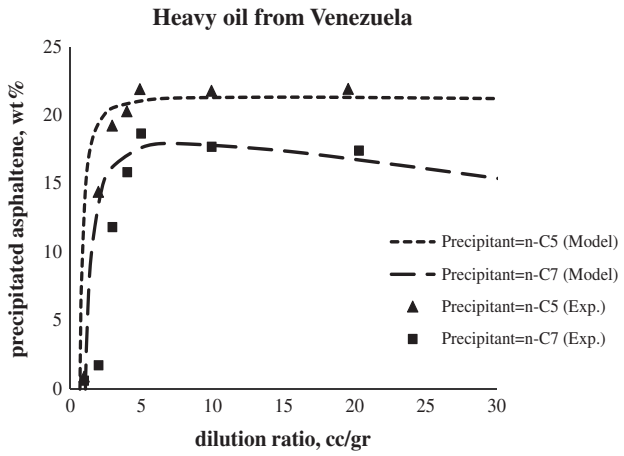

Fig. 14. Comparison of the PC-SAFT equation of state fitted and the experimental data for heavy oil from Venezuela. Experimental values are from Sabbagh et al. [21].

for modeling of heavy oils, the key point is using zero binary interaction parameters (*kij*) for asphaltenes, aromatics and resins components, except for *kij* between asphaltenes and saturates which needs to be a negative value. Zero and negative values for *kij* parameters of heavy oils are not uncommon. Also, comparison of asphaltenes' aromaticity and molecular weight of Iranian oil in Section 3.2 to those of heavy crudes in this section shows that Iranian crude which is light oil has a low aromaticity as well as low asphaltene molecular weight.

For the first time, this study shows the application of PC-SAFT for asphaltenes phase behavior modeling of heavy crudes and bitumens. Using polydispersity concept as well as zero *kij* parameters for asphaltenes component are the key points of titration experiments modeling of heavy crudes using PC-SAFT. Negative *kij* parameters between asphaltenes and saturates components can help to find a better match for the onset point and the shape of the curve right after precipitation onset.

4. Conclusions

This work provides a new insight into the polydisperse behavior of asphaltenes. In this article, the PC-SAFT equation of state is

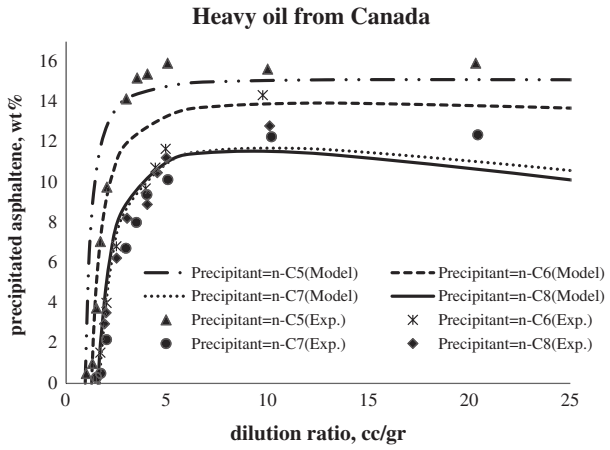

Fig. 15. Comparison of the PC-SAFT equation of state fitted and the experimental data for heavy oil from Canada. Experimental values are from Sabbagh et al. [21].

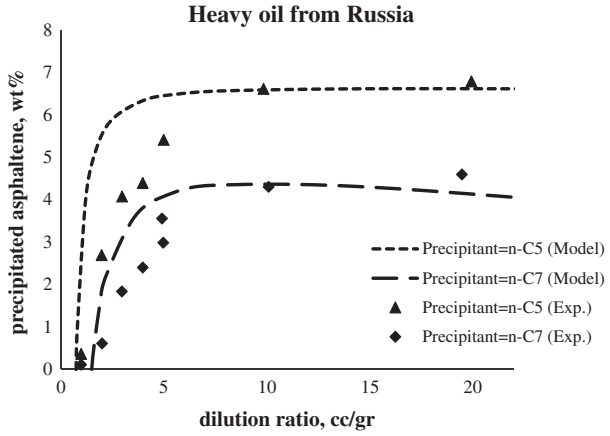

Fig. 16. Comparison of the PC-SAFT equation of state fitted and the experimental data for heavy oil from Russia. Experimental values are from Sabbagh et al. [21].

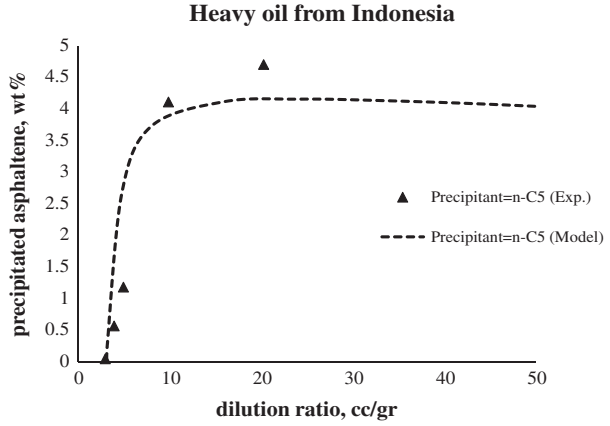

Fig. 17. Comparison of the PC-SAFT equation of state fitted and the experimental data for heavy oil from Indonesia. Experimental values are from Sabbagh et al. [21].

shown to reasonably model the phase stability of asphaltenes in crude oils diluted with *n*-alkanes. The asphaltenes and crude oils tested are from a variety of sources and over a wide range of oil density including heavy oils and bitumens. The following conclusions can be made from the investigations described in this paper.

Table 13
Binary interaction parameters between asphaltenes and saturates pseudo-components used for modeling of heavy oils and bitumens presented in Table 9.

Heavy oil source	*kij* Value between asphaltenes and Saturates
Venezuela	−0.009
Canada	−0.009
Russia	0.000
Indonesia	−0.008

- The proposed approach for selection of PC-SAFT parameters of polydisperse asphaltenes simplifies the process of parameter estimation by reducing the number of adjustable parameters.
- By treating asphaltenes as a polydisperse species, the amount of asphaltenes precipitated increases more gradually with precipitant addition than a monodisperse asphaltene species.
- Comparison of monodisperse and polydisperse asphaltenes modeling results showed that polydisperse asphaltenes re-dissolution begins at lower precipitant volume fractions and with a higher re-dissolution amount. The amount of re-dissolution is more for higher carbon number precipitant agents because they are better solvents for asphaltenes than lower carbon number *n*-alkanes.
- For polydisperse asphaltenes, near the initial asphaltenes instability onset, the precipitated phase is composed mostly of the heaviest asphaltenes fractions. As the amount of precipitant is increased further, lower molecular weight asphaltenes will also precipitate.
- Sensitivity analysis of model parameters shows that higher asphaltenes aromaticity along with lower asphaltenes molecular weight will result in fewer amounts of precipitated asphaltenes. This can be explained as an effect of the Flory–Huggins interaction parameter difference between light and heavy phases which is higher than the molar volume ratio difference.
- Heavy oil modeling results show that aromaticities of asphaltenes, aromatics and resins have a decreasing trend when stock tank oil density decreases. Higher aromaticity values show behavior closer to poly-nuclear-aromatics, and so a crude oil with higher aromaticity contains more amounts of poly-nuclear-aromatics fractions.
- Binary interaction parameters analysis show that the *kij* between asphaltenes and saturates fractions plays an important role in the modeling of both light and heavy crude oils diluted with *n*-alkanes. It can control the onset of precipitation as well as the shape of the titration curve right after the onset point.

Acknowledgements

The authors thank DeepStar and the R&D Oil Subcommittee of the Abu Dhabi National Oil Company for their financial support. The authors also thank Dr. Francisco M. Vargas for his valuable discussion about the polydisperse asphaltenes modeling.

References

[1] Hirschberg A, deJong LNJ, Schipper BA, Meijer JG. Influence of temperature and pressure on asphaltene flocculation. SPE J 1984;24:283–93.
[2] Alboudwarej H, Akbarzedeh K, Beck J, Svrcek WY, Yarranton HW. Regular solution model of asphaltene precipitation from bitumen. AIChE J 2003;49:2948–56.
[3] Panuganti SR, Vargas FM, Chapman WG. Modeling reservoir connectivity and tar mat using gravity-induced asphaltene compositional grading. Energy Fuels 2012;26:2548–57.
[4] Leontaritis KJ, Mansoori GA. Asphaltene flocculation during oil production and processing: a thermodynamic colloidal model. SPE 16258. In: SPE international symposium on oilfield chemistry, San Antonio, February 4–6 1987.
[5] Victorov AI, Firoozabadi A. Thermodynamic micellization model of asphaltene precipitation from petroleum fluids. AIChE J 1996;42:1753–64.

[6] Panuganti SR, Tavakkoli M, Vargas FM, Gonzalez DL, Chapman WG. SAFT model for upstream asphaltene applications. fluid phase equilibria; 2013; <http://dx.doi.org/doi:10.1016/j.fluid.2013.05.010>.
[7] Ting PD, Gonzalez DL, Hirasaki GJ, Chapman WG. Application of PC-SAFT equation of state to asphaltene phase behavior. In: Mullins OC, Sheu EY, Hammani A, Marshall AG, editors. Asphaltenes, heavy oils, and petroleomics. New York: Springer; 2007. p. 301–28.
[8] Victorov AI, Smirnova NA. Description of asphaltene polydispersity and precipitation by means of thermodynamic model of self-assembly. Fluid Phase Equilib 1999;158–160:471–80.
[9] Wang J, Buckley J. Effect of dilution ratio on amount of asphaltenes separated from stock tank oil. J Dispersion Sci Technol 2007;28:425–30.
[10] Panuganti SR, Vargas FM, Gonzalez DL, Kurup AS, Chapman WG. PC-SAFT characterization of crude oils and modeling of asphaltene phase behavior. Fuel 2012;93:658–69.
[11] Sedghi M, Goual L, Welch W, Kubelka J. Effect of asphaltene structure on association and aggregation using molecular dynamics. J Phys Chem B 2013;117:5765–76.
[12] Buckley JS, Hirasaki GJ, Liu Y, Von Drasek S, Wang JX, Gill BS. Asphaltene precipitation and solvent properties of crude oils. Pet Sci Technol 1998;16:251–85.
[13] Gonzalez DL, Hirasaki GJ, Chapman WG. Modeling of asphaltene precipitation due to changes in composition using the perturbed chain statistical associating fluid theory equation of state. Energy Fuels 2007;21:1231–42.
[14] Wang JX. Predicting asphaltenes flocculation in crude oils. Ph.D. thesis 2000. In: Petroleum and chemical engineering, New Mexico Institute of Mining and Technology. Socorro.
[15] Ting PD. Thermodynamic stability and phase behavior of asphaltenes in oil and of other highly asymmetric mixtures. Ph.D. thesis 2003. In: Chemical and Biomolecular Engineering, Rice University. Houston.
[16] Wiehe IA, Yarranton HW, Akbarzadeh K, Rahimi PM, Teclemariam A. The paradox of asphaltene precipitation with normal paraffins. Energy Fuels 2005;19:1261–7.
[17] Strausz OP, Safarik I, Lown EM, Morales-Izquierdo A. A critique of asphaltene fluorescence decay and depolarization-based claims about molecular weight and molecular architecture. Energy Fuels 2008;22:1156–66.
[18] Buenrostro-Gonzalez E, Lira-Galeana C, Gil-Villegas A, Wu J. Asphaltene precipitation in crude oils: theory and experiments. AIChE J 2004;50:2552–70.
[19] Wu J, Prausnitz JM, Firoozabadi A. Molecular thermodynamics of asphaltene precipitation in reservoir fluids. AIChE J 2000;46:197–209.
[20] Gonzalez DL. Modeling of asphaltene precipitation and deposition tendency using the PC-SAFT Equation of State. Ph.D. thesis 2008. In: Chemical and biomolecular engineering, Rice University. Houston.
[21] Sabbagh O, Akbarzadeh K, Badamchi-Zadeh A, Svrcek WY, Yarranton HW. Applying the PR-EoS to asphaltene precipitation from *n*-alkane diluted heavy oils and bitumens. Energy Fuels 2006;20:625–34.